Technical note: On seasonal variability of the M_2 tide

Richard D. Ray[1]

[1]Geodesy & Geophysics Lab., NASA Goddard Space Flight Center, Greenbelt, Maryland, USA

Correspondence: Richard Ray (richard.ray@nasa.gov)

Abstract. Seasonal variability of the M_2 ocean tide can be detected at many ports, perhaps most. Examination of the cluster of tidal constituents residing within the M_2 tidal group can shed light on the physical mechanisms underlying seasonality. In broadest terms these are astronomical, frictional/advective interactions, and climate processes; some induce annual modulations, some semiannual, in amplitude, phase, or both. This note reviews how this occurs and gives an example from each broad category. Phase conventions and their relationship to causal mechanisms, as well as nomenclature, are also addressed.

1 Introduction

It has long been noticed (Darwin, 1907; Corkan, 1934) that ocean tide constituents at some ports may experience significant seasonal variations. Especially noteworthy are large modulations discovered in some polar regions (e.g., Godin, 1986; Rotermund et al., 2021; Bij de Vaate et al., 2021). Significant modulations can also occur in lower latitudes, both regionally (Kang et al., 2002) and especially locally (e.g., Foreman et al., 1995). In fact, nearly all coastal tides show at least a small seasonal modulation (Pugh and Woodworth, 2014).

Climate-driven processes capable of inducing seasonal changes in barotropic tides are myriad: variability in ocean stratification (Müller, 2012), variability in ice cover (Prinsenberg, 1988), seasonal runoff and changes in river discharge (Guo et al., 2015), tide-surge interactions from predominantly wintertime storms (Pugh and Woodworth, 2014). Similar processes and others can induce seasonal perturbations in baroclinic tides detectable in surface measurements (Ray and Zaron, 2011; Zhao, 2021). The extent that the astronomical tidal potential plays in seasonality—usually small, but potentially important where tide amplitudes are large—is often overlooked. Some confusion on the issue has been recently clarified by Du and Yu (2021).

To help unravel observations it is useful to revisit the spectral characteristics behind seasonal variability. Understanding how certain spectral lines in observed sea level arise often points to possible physical mechanisms at work. The purpose of this note is to review this topic, focusing solely on the principal semidiurnal tide M_2. Much of what follows is hardly new; the purpose is to review and clarify, including even the nomenclature used. Whether seasonal variability is annual or semiannual, and whether it occurs in amplitude or phase or both, are obviously important aspects of variability; seeing one type of modulation rather than another can narrow the list of causes.

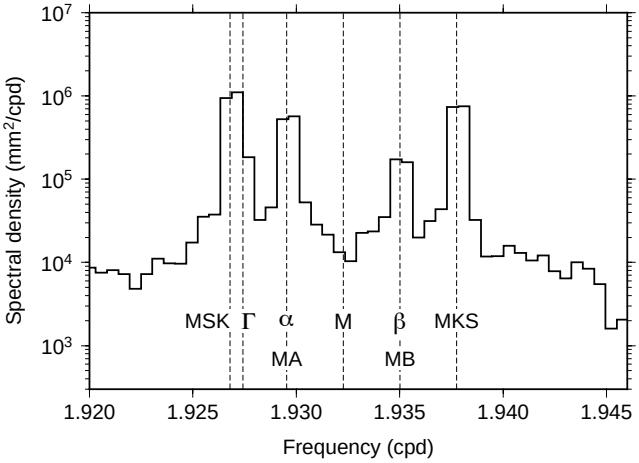

Figure 1. Spectrum of sea level at Saint-Malo, on the north coast of France, focusing on the M_2 group, but with the central M_2 constituent estimated and removed to better delineate the much smaller sidelines. The spectrum is based on 16 years of data. After spectral smoothing, the frequency resolution is approximately 0.2 cpy (or 0.0005 cpd), insufficient to clearly separate MSK_2 from Γ_2. The seasonal modulation of M_2 at Saint-Malo is evidently dominated by the two frictional compound tides, although α_2 is also important—see discussion in Section 3.2.

2 The M_2 tidal group

Recall the technical definitions (e.g., Munk and Cartwright, 1966) of 'tidal group'—a cluster of spectral lines with the same first two Doodson numbers—and 'tidal constituent'—a cluster with the same first three Doodson numbers. Tidal groups are separated in frequency by about 1 cycle per month, constituents by about 1 cycle per year. So when one speaks of seasonal variability of the M_2 tide, one must be speaking, in a sense, of the M_2 tidal group. It is the variability seen, for example, in a series of monthly estimates of M_2.

The main constituents within the M_2 group are listed in Table 1 in order of frequency. Included are tides generated by the astronomical potential (Cartwright and Edden, 1973; Hartmann and Wenzel, 1995), compound tides generated by shallow-water processes, and two annual sidelines (MA_2 and MB_2) commonly employed to effect an annual modulation from the wide range of possible climate processes. Climate processes are broadband, but they do commonly display a large spectral peak at once per year, and the two sidelines attempt to account for that. An example of these spectral lines in a real sea-level spectrum is shown in Fig. 1, computed from the tide-gauge measurements at Saint-Malo, France (and used further below).

Since all tides in the table are lunar, they all have 18.6-y nodal sidelines. These will be ignored in the present context, but they are obviously important for tidal prediction.

The constituent arguments given in the table are in the form of the standard mean longitudes that Doodson (1921) found so useful for ordering the whole tidal catalog. Simple expressions, linear in time for present-day tides, are readily available to evaluate the longitudes, and thus the tidal arguments, for any particular time (e.g., Pugh and Woodworth, 2014, p. 68).

Table 1. Tidal constituents within the M_2 group.

Constituent	Source	Argument	Freq. (deg/h)	Relative amp.
MSK_2	Friction	$2\tau - 2h$	28.901967	–
Γ_2	Gravitation	$2\tau - 2h + 2p + \pi$	28.911251	0.00301
MA_2	Climate	$2\tau - h$	28.943036	–
α_2	Gravitation	$2\tau - h + p' + \pi$	28.943038	0.00345
M_2	Gravitation	2τ	28.984104	1.00000
β_2	Gravitation	$2\tau + h - p'$	29.025171	0.00304
MB_2	Climate	$2\tau + h$	29.025173	–
δ_2	Gravitation	$2\tau + 2h$	29.066242	0.00114
MKS_2	Friction	$2\tau + 2h$	29.066242	–

τ – mean lunar time

h – mean longitude of sun

p – mean longitude of lunar perigee

p' – mean longitude of solar perigee, currently about 283°

All the tides of Table 1 differ in frequency from the central M_2 tide by either one or two cycles per year (cpy). They thus act to modulate the amplitude and/or phase of M_2 at those frequencies—the source, at least in spectral terms, of the seasonality of M_2. Most of the tidal arguments differ from M_2 by either $\pm h$ or $\pm 2h$, so the modulation is tied to the sun's declination, zero at the equinox; the speed of h is one cycle per tropical year. The two astronomical tides, α_2 and β_2, differ from M_2 by $\pm \ell'$ where $\ell' = h - p'$ is the sun's mean anomaly, zero at perihelion, so the modulation is tied to the sun's distance; the speed of ℓ' is one cycle per anomalistic year. The astronomical tide Γ_2 also depends on the position of the moon's perigee p. In an average sense, over many years, the contribution from Γ_2 to M_2 seasonality mostly cancels, because p (period 8.85 y) varies from one year to the next.

The frequencies of Table 1 are given with sufficient precision to show the tiny differences stemming from tropical versus anomalistic years, which are almost identical because the slowly moving p' requires 209 centuries to complete one revolution. So the annual pairs MA_2, MB_2 and α_2, β_2 take practically the same frequencies, and either pair may be used in a tidal analysis. But because their phases differ, the pairs cannot be interchanged; analysis and any subsequent prediction must maintain consistency.

Each class of constituent is now addressed in more detail.

2.1 Astronomical tides

The four gravitational sidelines are all very small, only about 0.3% of the primary, or smaller. With arguments depending on the mean longitude of the sun, they evidently arise from the sun's third-body perturbations of the lunar orbit. In particular, α_2, β_2 arise from what in lunar theory is called the "annual equation," which refers to an expansion or compaction of the moon's

orbit depending on whether the sun is at perihelion or aphelion, respectively. With a change in the orbital radius there is a corresponding change in the moon's angular velocity and thus longitude. The variation in longitude is given approximately by $-669'' \sin \ell'$ (Brouwer and Clemence, 1961, p. 329). The radial variation is $49 \cos \ell'$ km.

Because the ocean cannot support extremely high-Q resonances, the ocean's response (admittance) to gravitational forcing must be nearly constant across the small frequency band of the M_2 group. In that case, the gravitational components of the four sidelines can all be inferred from measurements of the central M_2 primary. Their amplitudes must be in the same proportion as the relative amplitudes of Table 1 and their phases must be nearly identical to the phase of M_2. It may be possible that this rule is violated in locations where large M_2 currents act through nonlinear dissipation to suppress the sidelines; this has been observed to happen for the M_2 nodal sideline (Ku et al., 1985).

Aside from this one exception, the induced seasonal modulations in M_2 from the astronomical sidelines are easily worked out. At a location with mean M_2 amplitude A and phase lag G, the combined elevation of the group is

$$\begin{aligned} \zeta_M(t) &= A\{\cos(2\tau - G) \\ &\quad + c_\alpha \cos(2\tau - \ell' + \pi - G) \\ &\quad + c_\beta \cos(2\tau + \ell' - G) \\ &\quad + c_\delta \cos(2\tau + 2h - G)\} \end{aligned}$$

where c_i are the relative amplitudes from Table 1, and the Γ_2 constituent has been dropped for reasons noted above. In analogy with the usual approach for handling nodal modulations, this expression may be written as a single modulated wave:

$$\zeta_M(t) = A\, f(t) \cos[2\tau - G + u(t)] \tag{1}$$

where functions f, u vary throughout the year as periodic functions of h (or ℓ'). Expanding the trigonometric functions and gathering like terms in $\cos G$ and $\sin G$ lead to

$$\begin{aligned} f \cos u &= 1 - (c_\alpha - c_\beta) \cos \ell' + c_\delta \cos 2h \\ f \sin u &= (c_\alpha + c_\beta) \sin \ell' + c_\delta \sin 2h \end{aligned} \tag{2}$$

or

$$f \approx 1 - 0.00041 \cos \ell' + 0.00114 \cos 2h \tag{3}$$

for the amplitude modulation, and

$$u \approx 0.372^\circ \sin \ell' + 0.065^\circ \sin 2h \tag{4}$$

for the phase modulation. The amplitude modulation is insignificant; because the main coefficients in (2) cancel, the second term from δ_2 is actually larger than the first term, but still very small. For the phase modulation in (4), the first term peaks at $\ell' = 90^\circ$, which is early April, and the smaller second term shifts that peak to mid-April. So the observed phase lag of M_2 (u

subtracts from G) takes its minimum value in mid-April and its maximum in mid-September. It is interesting to note that the first term in (4) is exactly twice the moon's longitude modulation of $669'' \sin \ell'$, alluded to above as arising from the annual equation in the sun's perturbation of the lunar orbit (it is twice, because M_2 is semidiurnal).

At most tide gauges, the gravitational components of any seasonal variability in the observed M_2 will thus comprise only a minor part. Observed variability will likely differ significantly from what might be inferred from the M_2 admittance or as modeled by Eqs. (3–4). Nonetheless, when only the astronomical modulation is important and the M_2 amplitude is moderately large, a phase modulation of 0.7° is easily seen; an example is given in Section 3.1.

2.2 Compound tides

Aside from the two compound tides listed in Table 1, there are possibly others that fall within the M_2 group (Simon, 2013). The most important is OP_2, exactly coinciding with MSK_2, and KO_2, exactly coinciding with M_2. The OP_2 and MSK_2 constituents likely arise from different nonlinear aspects of the hydrodynamics (Parker, 1991), although both are generated in shallow water.

The KO_2 tide is important only when M_2 is anomalously small; it can potentially induce an unusual nodal modulation (relative to the standard M_2 modulation), but it has no bearing on seasonality, with one exception: any seasonal variations in the primary K_1 or O_1 tides would induce seasonality in the compound KO_2, but cases where this is significant relative to M_2 must be rare. The few additional compound tides within the group noted by Simon (2013) are from interactions involving the diurnal S_1, which is normally small and will be ignored. Thus, when nonlinear shallow-water processes are acting sufficiently to produce a noticeable MSK_2 (or OP_2), the main effect of this will be equivalent to semiannual modulations in M_2 amplitude and/or phase.

2.3 Climate-induced modulations

The astronomical sidelines in Table 1 sit at discrete known frequencies. Compound tides are similar, although the number of them can sharply increase in shallow water. In contrast, climate-driven modulations are broadband. Although an annual cycle typically dominates, which is the justification for MA_2, MB_2, one might expect higher harmonics in some cases and also possibly a general smearing of observed spectral lines across the group (e.g., Munk et al., 1965).

Müller et al. (2014), building on an earlier study by Foreman et al. (1995), discussed the case of Victoria (Canada). There was a clear annual modulation in both amplitude and phase of M_2, but with an apparent second harmonic. Multi-year tidal analysis of the Victoria data (not shown) does show energy at the MSK_2 (or OP_2) frequency. Whether this is due to the compound tide(s) or to a true second harmonic below MA_2 is not clear. During tidal analysis it is sometimes possible to separate two constituents of identical frequency by exploiting their different nodal modulations (Parker et al., 1999), but in this case the amplitudes appear too weak to allow it.

The question of frictional compound tides versus higher harmonics of MA_2 and MB_2 is only one instance of the more general, and difficult, problem of deciphering the causes of climate-induced modulations, even when manifested by MA_2 or MB_2 acting alone (e.g., Pugh and Vassie, 1994).

2.4 Nomenclature

The constituent names in Table 1 follow both historical and current international conventions—for the latter, see the table maintained by the Tide, Water Level and Current Working Group of the International Hydrographic Organization.[1] The exception is β_2 which does not (yet) appear in the working group's table. Godin's 1988 book has the same usage as the IHO; his earlier 1972 book left the smaller lines unlabeled (Godin, 1972, 1988). Regarding β_2, however, it is commonly employed in the Earth tide community (e.g., Hartmann and Wenzel, 1995; Calvo et al., 2016; Ducarme and Schueller, 2018), and β_2 falls into the obvious pattern of using the first four letters of the Greek alphabet for the four astronomical constituents.

The two climate constituents apparently began as MA_2 and Ma_2 (Corkan, 1934). That lost favor, probably because a speaker cannot distinguish the two and also early computers employed only upper-case letters. MB_2 has been used for decades, at least in British work.[2] Amin (1976) still used Ma_2, but by 1983 he too had switched to MB_2.

Not included in Table 1 is the pair, H_1, H_2, for the two annual sidelines, which is starting to appear fairly often in the literature, probably because it is used in a popular open-source software package. The use of H_1 for a semidiurnal wave is certainly an oddity, as the tide community has used an integer subscript to denote tidal species since at least the end of the nineteenth century (Darwin, 1883; Harris, 1895; Cartwright, 1999). It is not clear where the symbol originated. An early (possibly first) use was by Pugh and Vassie (1976). Before that, in a discussion of shallow-water tides, Godin (1972, Table 2.14) used the label "(Horn)" for both sidelines and he cited a discussion by Horn (1960), although Horn himself left the lines unlabeled. Perhaps "(Horn)" has morphed into H_1, H_2, or the labels merely reflect the argument differences of $\pm h$. An important point, however, is that both Godin and Horn, as well as Pugh and Vassie, were referring to the two climate lines—none of their arguments involved p'—whereas the H_1, H_2 in present-day use are substituting for the gravitational tides α_2, β_2, as their arguments do involve p'. In any event, the use of a wrong subscript should be discouraged.

3 Three examples

In this section an example of M_2 seasonality arising from each of the three categories—gravitation, frictional interaction, and climate processes—is presented. For each tide gauge analyzed, a tidal solution based on a single inversion of many years of data was computed, sufficient to obtain reliable estimates of all constituents in Table 1. Based on an appropriate set of the estimated constituents (different for each category), the implied modulation of M_2 over one year was computed by complex demodulation. This is then compared with results of a second tidal inversion (or rather a set of inversions) in which estimates of M_2 were obtained for every month of the multi-year time series, from which monthly means were then computed. The monthly calculations accounted for the conventional 18.6-y nodal modulation of M_2, but no other modulations. (Standard errors in these monthly means were estimated from the standard deviations for each month, scaled by $1/\sqrt{n}$ for n years of data.)

[1] https://iho.int

[2] David Pugh has a copy of a November 1977 memorandum from David Cartwright, then director of the Bidston Observatory, proposing use of the modified symbols MA_2 and MB_2, in "deference to Corkan's original work." He suggested similar notation for other constituents affected by seasonal variability, such as NA_2, NB_2; these are now included in the IHO tables, as are MA_4, MB_4.

Table 2. Amplitude, Greenwich phase lag, and dimensionless admittance for the M_2 group at Port Orford, Oregon

Tide	A (cm)	G (°)	$\lvert Z\rvert$
MSK_2	0.03	52.2	–
Γ_2	0.24	218.1	1.24 ± 0.20
α_2	0.27	198.4	1.24 ± 0.18
M_2	74.70	216.5	1.18 ± 0.00
β_2	0.19	205.2	0.98 ± 0.20
δ_2	0.08	199.4	1.12 ± 0.40

The goal is to confirm that seasonality of M_2, as delineated by monthly mean estimates of amplitude and phase, can—at least in these cases—be accurately reproduced by the modulations from a particular set of spectral lines. Which lines are in play differ depending on the category of causation.

3.1 Astronomical modulations

It is actually not easy to find good examples of seasonal variability stemming solely from the purely astronomical constituents of Table 1. Any potential case must display fairly constant admittances across the group of gravitational constituents. Yet at most tide gauges one sees perturbations in the admittance, or one sees significant amplitudes in the compound tides.

The time series at Port Orford, Oregon, is one of the better examples. Tidal constants estimated from 26 years of data[3] (1994–2021) are listed in Table 2. The magnitudes of tidal admittances $|Z|$ are all consistent within error limits, all phases are close, and the compound MSK_2 is very small. Combining the harmonic constants of the three astronomical constituents $\alpha_2, \beta_2, \delta_2$ implies a seasonal modulation of M_2 given by the solid lines of Fig. 2. These are in good agreement with the monthly mean estimates, aside perhaps for the January amplitude.

The theoretical seasonal modulations, based on Eqs. (3–4) are shown as the dashed lines. The solid and dashed lines agree well in phase, less well in amplitude, at first glance. But note that the amplitude vertical axis spans only 1 cm, so in fact the amplitude agreement is also quite good, with all data implying very little amplitude modulation. The small differences in amplitude curves occur because the estimated admittances in Table 2 are not identical, simply due to unavoidable estimation error.

The analysis at Port Orford confirms that the astronomically induced seasonal modulation of M_2 results in almost no amplitude modulation, and a phase modulation of about 0.7°, with a minimum in April and maximum in September.

[3]Data at Port Orford are available from 1978 to present, but the data before 1994 yield tidal estimates too erratic to use. Data after 1993 appear of good quality.

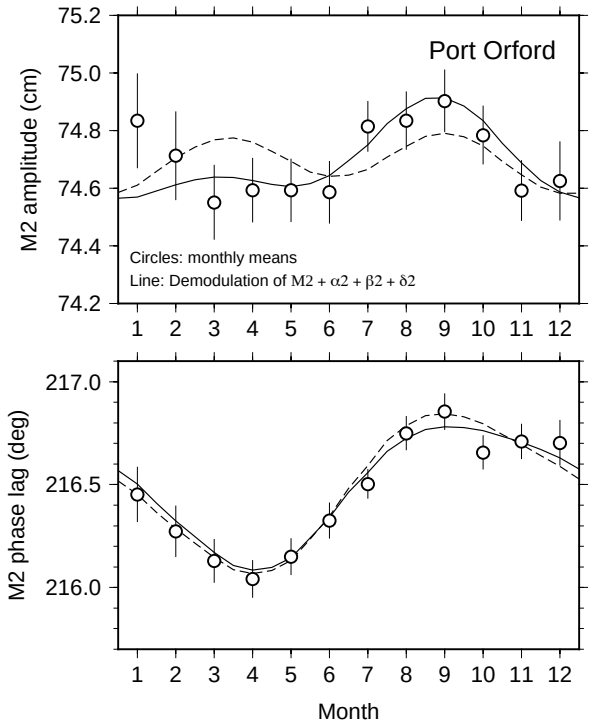

Figure 2. Seasonal variations in M_2 amplitude (top) and Greenwich phase lag (bottom) observed at Port Orford, Oregon. Circles with error bars are based on monthly mean M_2 estimates from 26 years of hourly data. The solid lines are the implied seasonal variations from the estimated side-constituents $\alpha_2, \beta_2, \delta_2$. The dashed lines are a theoretical seasonal modulation based on Eqs. (3–4). Note the amplitude axis spans only 1 cm.

3.2 Frictional/advective modulations

An example of modulations dominated by one or both of the compound tides in the M_2 group is Saint-Malo, France, whose spectrum was shown in Fig. 1. The two annual constituents (α_2, β_2 or MA_2, MB_2) are smaller, as the spectrum reveals, but still too large to ignore. The total modulation, based on four constituents, is shown in Fig. 3. The amplitude clearly reveals the presence of a semiannual modulation, with a slow rise during the beginning of the year, then a rapid decay between July and October. The phase is dominated by the semiannual effect, with an annual contribution responsible for the September phase lag exceeding the earlier peak in March.

3.3 Annual climate modulations

Tide gauges with annual variations in M_2, and thus with sidelines dominated by MA_2 and/or MB_2 are easy to find. The case of Victoria was already noted (Müller et al., 2014), partly for having a second harmonic in its modulation. However, there are many tide gauges where only the annual modulation presents itself. A fair number can be found along the coast of Japan, even

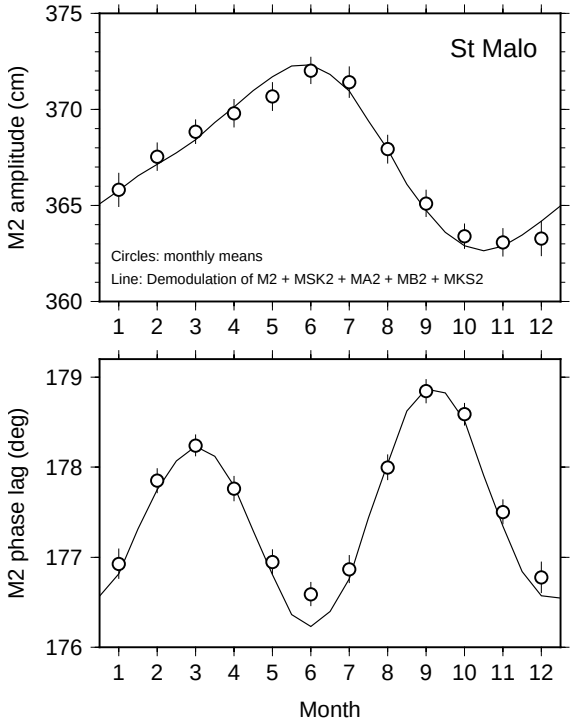

Figure 3. Similar to Fig. 2, but for Saint-Malo, France. The solid line is here based on demodulation of four tidal sidelines, the two annual constituents MA_2, MB_2 and the two compound constituents MSK_2, MKS_2. The latter dominate according to the spectrum shown in Fig. 1 and thus result in the clear semiannual modulation of the M_2 phase.

though M_2 itself is not especially large there. The example chosen here is in fact one of the largest modulations discovered anywhere: Chittagong, along the coast of Bangladesh. At that location the annual sea level term, Sa, is also anomalously large, presumably reflecting large discharge from the Ganges. Several other nearby tide gauges, with somewhat smaller M_2 modulations, were studied by Tazkia et al. (2017).

Harmonic analysis of eleven years of hourly data (2008–2018) at Chittagong reveals astonishing large amplitudes for MA_2 and MB_2 of 15.5 and 10.1 cm, respectively, with the M_2 constituent at 171.6 cm. The resulting seasonal modulation is shown in Fig. 4. The monthly mean amplitudes range from 146 cm in February to a high of 195 cm in August. In comparison, the phase modulation is not very large, about 4°. The monthly mean phases appear slightly erratic and fit the demodulated curve only moderately well.

The large modulation in amplitude at this location closely mimics the large oscillation in annual sea level, which is minimum in February and maximum in July, with a mean range of 71 cm. Tazkia et al. (2017) developed a tide model for the region that explores this interdependence.

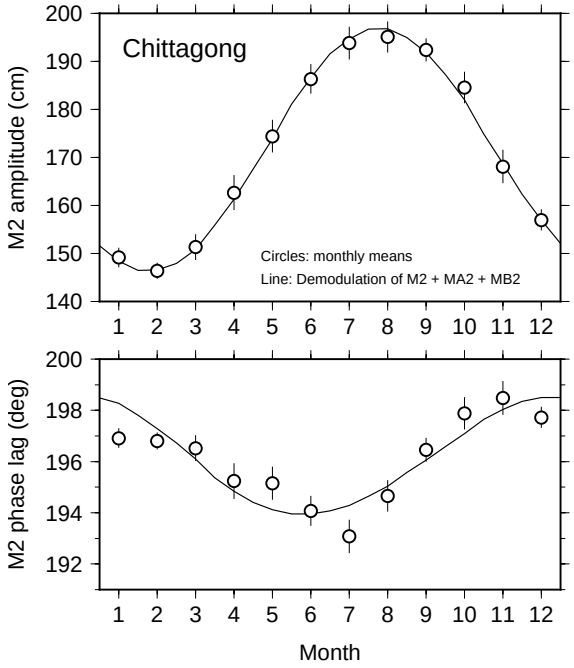

Figure 4. Similar to Fig. 2, but for Chittagong, along the coast of Bangladesh, east of the Ganges Delta. The unusually pronounced modulation of the M_2 amplitude at this location mimics the usually large annual oscillation of sea level, both having a minimum in February and maximum in July/August.

4 Conclusions

One indication of the variety of processes responsible for seasonal variability of the M_2 tide is the variety of different mechanisms generating spectral lines within the M_2 group: astronomical motions of the moon, frictional and other nonlinear interactions between tidal waves, and climate processes. The astronomical contribution is predictable given good long-term mean estimates of the M_2 constants; it is mostly a $\pm 0.37^\circ$ modulation in phase, precisely double the solar perturbation in the moon's longitude arising from the "annual equation" of lunar theory. On the other hand, when a tide gauge is found to be affected by substantial seasonality in M_2, it usually arises from one or both of the constituents MA_2, MB_2. The variety of climate processes responsible for those two constituents—annual changes in stratification, sea level, ice cover, etc.—is where the real complication lies when attempting to understand seasonal variability.

Data availability. The Port Orford and Chittagong tide gauge data are available from the University of Hawaii Sea Level Center. The Saint-Malo tide gauge data are available from Le SHOM, the French national hydrographic service.

Competing interests. The author has no competing interests.

Acknowledgements. It is a pleasure to thank Philip Woodworth and David Pugh for discussions. This work was supported by the U.S. National Aeronautics and Space Administration through the Sentinel-6 and Sea Level Change projects.

References

Amin, M.: The fine resolution of tidal harmonics, Geophys. J. R. astr. Soc., 44, 293–310, 1976.

Bij de Vaate, I., Vasulkar, A. N., Slobbe, D. C., and Verlaan, M.: The influence of Arctic landfast ice on seasonal modulation of the M_2 tide, J. Geophys. Res.: Oceans, 126, e2020JC016 630, https://doi.org/10.1029/2020JC016630, 2021.

Brouwer, D. and Clemence, G. M.: Methods of Celestial Mechanics, Academic Press, New York, 1961.

Calvo, M., Rosat, S., and Hinderer, J.: Tidal spectroscopy from a long record of superconducting gravimeters at Strasbourg, in: International Symposium on Earth Sciences for Future Generations, edited by Freymueller, J. et al., pp. 131–136, Springer, https://doi.org/10.1007/1345_2016_223, 2016.

Cartwright, D. E.: Tides: A Scientific History, Cambridge Univ. Press, Cambridge, 1999.

Cartwright, D. E. and Edden, A. C.: Corrected tables of tidal harmonics, Geophys. J. R. astr. Soc., 33, 253–264, 1973.

Corkan, R. H.: An annual perturbation in the range of tide, Proc. Royal Soc., 144, 537–559, 1934.

Darwin, G. H.: The harmonic analysis of tidal observations, British Association Report for 1883, pp. 49–118, reprinted in Darwin's *Scientic Papers*, vol. 1, 1–70, Cambridge Univ. Press, 1907, 1883.

Darwin, G. H.: On the Antarctic tidal observations of the 'Discovery', in: Scientific Papers. Volume 1: Oceanic Tides and Lunar Disturbance of Gravity, pp. 372–388, Cambridge Univ. Press, 1907.

Doodson, A. T.: The harmonic development of the tide-generating potential, Proc. Royal Soc., 100, 305–329, 1921.

Du, Z. and Yu, Q.: Comment on "Seasonal and nodal variations of predominant tidal constituents in the global ocean" by Cao et al., Cont. Shelf Res., 227, 104 524, https://doi.org/10.1016/j.csr.2021.104524, 2021.

Ducarme, B. and Schueller, K.: Canonical wave grouping as a key to optimal tidal analysis, Marees Terr. Bull. Inf., 150, 12 131–12 244, http://www.bim-icet.org, 2018.

Foreman, M. G. G., Walters, R. A., Henry, R. F., Keller, C. P., and Dolling, A. G.: A tidal model for eastern Juan de Fuca Strait and the southern Strait of Georgia, J. Geophys. Res., 100, 721–740, 1995.

Godin, G.: The Analysis of Tides, University of Toronto Press, Toronto, 1972.

Godin, G.: Modification by an ice cover of the tide in James Bay and Hudson Bay, Arctic, 39, 65–67, 1986.

Godin, G.: Tides, CICESE, Ensenada Baja California, Mexico, 1988.

Guo, L., van der Wegen, M., Jay, D. A., Matte, P., Wang, Z. B., Roelvink, D., and He, Q.: River-tide dynamics: exploration of nonstationary and nonlinear tidal behavior in the Yangtze River estuary, J. Geophys. Res.: Oceans, 120, 3499–3521, https://doi.org/10.1002/2014JC010491, 2015.

Harris, R. A.: Manual of tides. Part III., in: Report of the Superintendent, U.S. Coast and Geodetic Survey, Part II., pp. 125–262, U. S. Gov't. Printing Office, Washington, 1895.

Hartmann, T. and Wenzel, H.-G.: The HW95 tidal potential catalogue, Geophys. Res. Lett., 22, 3553–3556, 1995.

Horn, W.: Some recent approaches to tidal problems, Int. Hydrogr. Rev., 37, 65–88, 1960.

Kang, S. K., Foreman, M. G. G., Lie, H.-J., Lee, J.-H., Cherniawsky, J., and Yum, K.-D.: Two-layer tidal modeling of the Yellow and East China Seas with application to seasonal variability of the M_2 tide, J. Geophys. Res., 107, 3020, https://doi.org/10.1029/2001JC000838, 2002.

Ku, L.-F., Greenberg, D. A., Garrett, C. J. R., and Dobson, F. W.: Nodal modulation of the lunar semidiurnal tide in the Bay of Fundy and Gulf of Maine, Nature, 230, 69–71, 1985.

Müller, M.: The influence of changing stratification conditions on barotropic tidal transport and its implications for seasonal and secular changes of tides, Cont. Shelf Res., 47, 107–118, https://doi.org/10.1016/j.csr.2012.07.003, 2012.

Müller, M., Cherniawsky, J. Y., Foreman, M. G. G., and von Storch, J.-S.: Seasonal variation of the M_2 tide, Ocean Dynam., 64, 159–177, https://doi.org/10.1007/s10236-013-0679-0, 2014.

Munk, W. H. and Cartwright, D. E.: Tidal spectroscopy and prediction, Phil. Trans. Royal Soc., A259, 533–581, 1966.

Munk, W. H., Zetler, B., and Groves, G. W.: Tidal cusps, Geophys. J. R. astr. Soc., 10, 211–219, 1965.

Parker, B. B.: The relative importance of the various nonlinear mechanisms in a wide range of tidal interactions (review), in: Tidal Hydrodynamics, edited by Parker, B. B., pp. 237–268, John Wiley, New York, 1991.

Parker, B. B., Davies, A. M., and Xing, J.: Tidal height and current prediction, in: Coastal Ocean Prediction, edited by Mooers, C. N. K., pp. 277–327, American Geophysical Union, Washington, 1999.

Prinsenberg, S. J.: Damping and phase advance of the tide in western Hudson Bay by the annual ice cover, J. Phys. Oceanogr., 18, 1744–1751, 1988.

Pugh, D. T. and Vassie, J. M.: Tide and surge propagation off-shore in the Dowsing region of the North Sea, Dt. Hydrogr. Z., 29, 163–213, 1976.

Pugh, D. T. and Vassie, J. M.: Seasonal modulations of the principal semidiurnal lunar tide, in: Mixing and Transport in the Environment: A Memorial Volume for Catherine Allen, edited by Beven, K. J. et al., chap. 13, pp. 247–267, John Wiley, 1994.

Pugh, D. T. and Woodworth, P. L.: Sea Level Science: Understanding Tides, Surges, Tsunamis and Mean Sea-Level Changes, Cambridge Univ. Press, Cambridge, 2014.

Ray, R. D. and Zaron, E. D.: Non-stationary internal tides observed with satellite altimetry, Geophys. Res. Lett., 38, L17609, https://doi.org/10.1029/2011GL048617, 2011.

Rotermund, L. M., Williams, W. J., Klymak, J. M., Wu, Y., Scharien, R. K., and Haas, C.: The effect of sea ice on tidal propagation in the Kitikmeot Sea, Canandian Arctic archipelago, J. Geophys. Res.: Oceans, 126, e2020JC016 786, https://doi.org/10.1029/2020JC016786, 2021.

Simon, B.: Coastal Tides, Institut Océanographique, Monaco, 2013.

Tazkia, A. R., Krien, Y., Durand, F., Testut, L., Papa, F., and Bertin, X.: Seasonal modulation of M2 tide in the northern Bay of Bengal, Cont. Shelf Res., 137, 154–162, https://doi.org/10.1016/j.csr.2016.12.008, 2017.

Zhao, Z.: Seasonal mode-1 M_2 internal tides from satellite altimetry, J. Phys. Oceanogr., 51, 3015–3035, https://doi.org/10.1175/JPO-D-21-0001.1, 2021.